Pharmaceutical Dry Powder Aerosols: Correlation of Powder Properties with Dose Delivery and Implications for Pharmacodynamic Effect

Neville M. Concessio,[1,2,5] Michiel M. VanOort,[3] Michael R. Knowles,[4] and Anthony J. Hickey[1]

Received December 2, 1998; accepted March 9, 1999

Purpose. Efficient dispersion of bulk solids is critical for dry powder aerosol production which can be viewed as a sequence of events from stationary through dilated, flowing and finally dispersed particulates. The purpose of this study was to test the hypothesis that numerical descriptors of powder flow properties predict aerosol dispersion and pharmacodynamic effect.

Methods. Drug and excipient particles were prepared in size ranges suitable for inhalation drug delivery, and their physico-chemical properties were evaluated. Novel techniques (chaos analysis of dynamic angle of repose and impact force separation) were developed and utilized to measure and characterize powder flow and particle detachment from solid surfaces, respectively. Dry powder aerosol dispersion was evaluated using inertial impaction. Pharmacodynamic evaluations of bronchodilation were performed in guinea pigs, for selected formulations.

Results. We observed a direct correlation of powder flow with ease of particle separation (r^2 = 0.9912) and aerosol dispersion (r^2 = 0.9741). *In vivo* evaluations indicated that formulations exhibiting a higher *in vitro* dose delivery resulted in a greater reduction in pulmonary inflation pressure.

Conclusions. These results integrate powder behavior at various levels and indicate that numerical descriptors of powder flow accurately predict dry powder aerosol dispersion. A proportionality between aerosol dispersion and pharmacodynamic effect was observed in preliminary *in vivo* evaluations, which demonstrates the potential of these techniques for correlation studies between *in vitro* powder properties and *in vivo* effect.

KEY WORDS: dry powder aerosols; powder flow; capacity dimension; impact force separation; dispersion; pharmacodynamic effect; bronchodilation.

INTRODUCTION

The requirement for viable alternatives to ozone-depleting metered dose inhalers (MDIs), coupled with the opportunity for local airway and systemic delivery of new therapeutic agents, make dry powder aerosols an attractive choice for inhalation drug delivery. Thus, the traditional use of aerosols for local airway diseases can be extended to treat a variety of pulmonary and systemic disorders, including genetic diseases. However, it is critical that the mechanisms of particle dispersion be better defined, and correlated with *in vivo* delivery and effects, if optimization of dry powder aerosol delivery is to be achieved.

Traditional aerosol devices include commercially available pressure-packaged metered dose inhalers (MDIs), nebulizers and dry powder inhalers (DPIs) (1). DPIs are an alternative to propellant-driven systems which overcome the breath coordination problems associated with MDIs, but there are significant limitations in the current technology for dry powder dispersion. Particle size is the principal factor influencing lung deposition (2,3). The majority of commercially available DPIs consist of micronized drug powder (<5 μm) blended with larger (~30–90 μm) inert carrier particles (usually α-lactose monohydrate) (4,5). Micron sized particles exhibit forces of attraction, primarily dictated by Van der Waals, electrostatic and capillary forces (6,7), which are affected by the size, shape and chemical composition of the particle. These forces contribute to particle-particle and particle-surface interactions. Attempts to predict and manipulate powder flow and dispersion by controlling and evaluating each individual force have met with limited success. Further understanding and improvements in dry powder dispersion are critical if DPIs are to consistently compete with, or surpass, the performance of propellant driven systems.

The complex interplay of the forces of dispersion may be best addressed by testing the behavior of the whole system, namely powder flow and dispersion. The development and evaluation of novel techniques for measuring and analyzing particle detachment and dynamic powder flow are described. Studies were performed to test the hypothesis that numerical descriptors of powder flow properties predict aerosol dispersion, *in vitro*, which would then correlate with pharmacodynamic effect, *in vivo* (8).

MATERIAL AND METHODS

Materials

Albuterol sulfate, a β_2-adrenergic agonist was selected as the model drug. Lactose and maltodextrin were employed as carrier particles, and sodium chloride was a reference powder. Albuterol sulfate was donated by GlaxoWellcome Inc., RTP, NC; maltodextrin by Grain Processing Corp., Muscatine, IA; lactose was obtained from Pharmatose, Fraser, NY; and sodium chloride from Mallinckrodt Chemical Works, St. Louis, MO.

Particle Preparation and Characterization

Micronized drug particles <5 μm were prepared by jet milling (9) [Trost Impact Pulverizer, Garlock Inc., Plastomer Products, Newton, PA], and larger excipient particles (≥45 μm)

[1] Division of Pharmaceutics, School of Pharmacy, University of North Carolina, Chapel Hill, North Carolina 27599.
[2] Present address: Pharmaceutical Division, Biotechnology, Bayer Corporation, 800 Dwight Way, Berkeley, California 94710.
[3] Inhalation Product Development, GlaxoWellcome Inc., RTP, North Carolina 27709.
[4] Cystic Fibrosis Pulmonary Research and Treatment Center, University of North Carolina, Chapel Hill, North Carolina 27599.
[5] To whom correspondence should be addressed. (e-mail: neville.concessio.b@bayer.com).

ABBREVIATIONS: CMD, count median diameter; DPI, dry powder inhaler; FPM, fine particle mass; GSD, geometric standard deviation; HDE, highest dosing efficiency formulation (2% albuterol sulfate in 45–75 μm lactose); LDE, lowest dosing efficiency formulation (1% albuterol sulfate in 75–125 μm maltodextrin); MDI, metered dose inhaler; N, newton, kg.m/s^2; PIP, pulmonary inflation pressure; θ, dynamic angle of repose; $\bar{\theta}$, average dynamic angle of repose; $d\theta$, $\theta - \bar{\theta}$.

0724-8741/99/0600-0828$16.00/0

were prepared in narrow size ranges by sieving (9) using a vibrating 3-inch sieve shaker (Gilson Co. Inc., Worthington, OH). Micronized albuterol sulfate (<5 μm) was blended with excipients (lactose, maltodextrin or sodium chloride) in the 45–75 and 75–125 μm size range in a Turbula mixer (10) [GlenMills Inc., Clifton, NJ] at 20 rpm.

The particle size and distribution, static angle of repose, moisture content, density and surface area of the above powders were evaluated. Particle size was evaluated using two techniques; scanning electron microscopy with image analysis and laser diffraction. Image analysis (Sigma Scan®, Jandel Scientific, Corte Madera, CA) of photomicrographs obtained by scanning electron microscopy (JEOL 6300, JEOL Corp., Peabody, MA) was used to estimate the particle size distribution based on the estimated projected area of the particle of interest ($n \geq 500$), which is the diameter of a circle having the same area as the estimated projected area of the particle of interest. Photomicrographs of each powder were obtained from a minimum of 10 different fields. Unobstructed particles in full view were counted with an average of 50 measurements per field. The median particle size (count median diameter, CMD) and geometric standard deviation (GSD) were obtained from plots of the logarithm of particle size versus the frequency on a probability scale. The CMD is the diameter equivalent to a cumulative frequency of 50%, whereas the GSD, representing the distribution around the median diameter, is calculated by dividing the particle size corresponding with the cumulative frequency associated with one standard deviation from the mean by the median diameter [$GSD = d_{84\%}/d_{50\%}$]. Replicate measurement ($n = 5$) of particle size distributions were also performed by laser diffraction using a RODOS powder disperser and a BA Helos laser diffraction system (Sympatec, GmbH, Germany). The static angle of repose, defined as the maximum angle possible between the side of the powder heap and the horizontal plane, was measured by the poured angle method (11). Bulk density was determined by pouring 50 g of powder into a 100 ml glass graduated cylinder and measuring the volume occupied. Tapping the cylinder till the powder settled to a constant volume was used to calculate the tapped density. The moisture content was determined by a moisture balance analyzer (model LJ16, Mettler Toledo, Fisher Scientific, Atlanta, GA) used to heat the sample to a constant weight. The surface area of powders was determined by measuring the gas adsorbed as a monolayer onto the powder surface (Quantachrome Autosorb 1, Quantachrome Corp., Syosset, NY).

Powder Flow

Most powders are complex systems exhibiting irregular flow and dispersion properties (9,12,13), reflecting the influence of a combination of interactive forces on the system. Powder flow properties were evaluated by dynamic angle of repose (θ) evaluations coupled with novel chaos data analysis (12,14), to characterize underlying order in pharmaceutical powders and to describe flow by a single numerical descriptor. The angle between the powder bed and the horizontal, defined as the dynamic angle of repose (θ), was determined as the powder bed (10 g) was allowed to rise and cascade down the sides of a stainless steel drum (8.5 inches in diameter and 2.25 inches deep) rotating at 0.5 rpm. The nature of the powder, whether cohesive or free flowing, caused the powder bed to rise and fall to varying heights in the rotating drum. A video camera (VHS model AG-160, Panasonic, Japan) was used to capture images of the powder behavior which were played back on a video recorder (model AG-1270P, Panasonic, Japan) and viewed on a television monitor (GE monitor, IN), at 50 frames/sec. Measurements of θ ($n > 1000$)were performed every 100 ms (15) [$n = 3$]. The average ($\bar{\theta}$) was calculated and the difference, $d\theta = \theta - \bar{\theta}$, was plotted versus time.

The resulting oscillating data were interpreted utilizing several techniques (13,15); ultimately a single numerical descriptor, the capacity dimension was used to quantify flow. Phase-space plots (16,17) employed in the present studies were two-dimensional plots in which the derivative $d\theta'$ [$d\theta' = d(d\theta)/dt$] was plotted versus $d\theta$ [$d\theta = \theta - \bar{\theta}$], at each data point. Phase-space plots are commonly quantified by calculating various dimensions which measure the complexity of the phase-space trajectory (18,19). In the present studies the capacity dimension, defining the spread of trajectories in phase-space, was determined by the box counting method (19). The phase-space was divided successively into equal boxes or cubes of known dimensions. The fraction of the cubes that were occupied with data points was determined. The log of the fraction of cubes occupied by data points was plotted versus the log of the linear dimension of the cubes, and the capacity dimension was determined from the slope of the line.

The capacity dimension is defined by the following equation,

$$CD = \lim_{\epsilon \to 0} \frac{\log N(\epsilon)}{\log(1/\epsilon)}$$

where $N(\varepsilon)$ is the number of cubes, whose sides have length ε, that are necessary to cover the attractor.

Particle Detachment from Solid Surfaces

The adhesive and cohesive forces affecting powder flow also cause drug and excipient particles to adhere to solid surfaces resulting in poor dose delivery from DPIs. This force of adhesion can be determined by measuring the force required to separate particles from a surface.

A pendulum type impact force separation device, based on the design of Otsuka *et al.* (20), was constructed of stainless steel and consisted of a pendulum arranged with a hammer head capable of impinging on a vertically mounted sapphire disc (Edmund Scientific, NJ). The impact acceleration of the pendulum at the hammer head was measured by using a piezoelectric accelerometer (model PEL, Sensotec, Columbus, OH). The force of impact ($kg.m/s^2$ or N) was calculated from the product of the impact acceleration (m/s^2) and the mass of the hammer head (kg). The powder evaluated was uniformly coated on a sapphire disc which was subjected to various impact forces. Microscopy (Nikon SMZ U, Tokyo, Japan) with image analysis (Sigma Scan®, Jandel Scientific, Corte Madera, CA) was used to determine the median size (CMD) and distribution (GSD) of excipient particles adhered to the disc following impact ($n = 5$).

Aerosol Dispersion and *In Vitro* Aerodynamic Characterization

Dispersion properties of drug:excipient blends were evaluated from the Rotahaler® (GlaxoWellcome, Inc., NC), a passive

device commercially available for the delivery of albuterol sulfate (21). Dose delivery and fine particle mass (FPM, the mass of drug in the respirable size range [≤5 μm] capable of penetrating and depositing in the lower lung) of 2% w/w albuterol sulfate blends with lactose, maltodextrin or sodium chloride (45–75 and 75–125 μm) were evaluated by inertial impaction. The Andersen cascade impactor (Graseby Inc., Smyrna, GA), is a multistage, multi-orifice impactor, consisting of a preseparator, eight collection stages and a backup filter (22,23). The method prescribed for DPI clinical use involves inhaling at a high flow rate through the device and subsequent breath holding (24). The cut-off for the eight stages in the Andersen impactor have been recalculated and calibrated for higher flow rates (25), and for a physiologically relevant flow rate of 60 L/min they are 6.18, 3.98, 3.23, 2.27, 1.44, 0.76, 0.48, and 0.27 μm. Unit doses (50 mg) of drug:excipient blends (2% w/w) were filled in size 3 gelatin capsules (Eli Lilly and Co., IN), and generated and sampled at 60L/min for a period of 3s. The impaction surfaces were coated with silicone oil to minimize inter-stage losses due to particle bounce. Following aerosolization, the stages were washed and albuterol sulfate was analyzed by a high pressure liquid chromatography assay with U.V. detection at 276 nm. FPM values were obtained from a fitting procedure based on a 5 μm cut-off.

Statistical Experimental Design

The final objective of this study was to correlate *in vitro* dose delivery of selected formulations to pharmacodynamic effect. The variables affecting *in vitro* dose delivery are numerous. Therefore, a half fraction of a complete 2 factorial design was utilized to evaluate the effect of five factors, each at 2 levels, on dose delivery and to identify extremes of dose delivery for subsequent *in vivo* evaluations. The five factors evaluated were the excipient (lactose, maltodextrin), size range of excipient (45–75, 75–125 μm), drug concentration in blend (1%, 2% w/w), delivery device (Rotahaler®, Pfeiffer [26]) and sampling flow rate through the impactor (60, 90 L/min). The Andersen 8-stage cascade impactor was used to size characterize the powder formulations generated as an aerosol, as described previously. Formulations exhibiting the highest and lowest dosing efficiency were also identified for *in vivo* pharmacodynamic evaluation.

Pharmacodynamic Evaluation

The guinea pig may be utilized as a model to evaluate pulmonary conditions such as allergen-induced bronchoconstriction (27), and for the action of anti-asthmatic drugs (28). The use of a bronchodilator drug, albuterol sulfate, allowed pharmacodynamic evaluation of bronchodilation in guinea pigs. A 4 × 4 Latin square experimental design was adopted for evaluating selected formulations at equivalent unit doses (100 μg), and excipient controls on induction of bronchodilation in guinea pigs (n = 16) [UNC-CH, IACUC Protocol No. 97-119.0-A, entitled, 'Evaluation of Novel Dry Powder Aerosol Preparations of Albuterol Sulfate']. The experiments performed adhered to the 'Principles of Laboratory Animal Care' (NIH Publication #85-23, revised 1985).

The experimental apparatus followed the Konzett Roessler arrangement (29). Dunkin Hartley guinea pigs (female, 350–400 g) were anesthetized with 0.875 ml/Kg of a 0.75:0.05:0.075 Ketamine (100 mg/mL): Xylazine (100 mg/mL): Acepromazine (10 mg/mL) mixture administered IM, tracheostomized, and intubated to allow positive pressure ventilation of 5.0 ml air/breath at 60 breaths/min (Model 683, Harvard Apparatus, South Natick, MA). Depth of anesthesia was assessed by loss of corneal reflex and lack of response to interdigital pinch. The body temperature of the animal was maintained at 37°C. A bronchospasm transducer (model 7020, Ugo Basile, Italy) (30) was connected to a side arm, and employed to measure pulmonary inflation pressure as an indication of airway resistance. A stable baseline pulmonary pressure was established prior to intratracheal administration of drug/excipient particles, using a dry powder insufflator (Penn Century, Philadelphia, PA). The insufflator consists of an L-shaped 18 gauge needle attached to the sample chamber which serves as the delivery tube for the aerosolized powder formulation into the guinea pig trachea. The powder was inserted into the sampling chamber of the device, and quantified by weighing the device before and after sample loading, and following sample discharge. A mechanical air supply from a 3 ml syringe delivered the force required to disperse the drug formulation. Changes in pulmonary inflation pressure (PIP), measured by the bronchospasm transducer, were monitored by a data acquisition software package (Windaq, Dataq Instruments, Columbus, OH).

Unit dose delivery and uniformity (n = 5) of selected formulations were evaluated using an MDI unit dosage sampling apparatus (Nephele Enterprises, White Bear Lake, MN) at a flow rate of 60 L/min. The device consisted of a Teflon tube and filter assembly holding a 0.22 μm filter. Individual doses were actuated into the device which was washed and analyzed for drug content to determine the dose recovery from the device.

RESULTS AND DISCUSSION

Particle Preparation and Characterization

Table I shows the particle size and distribution as evaluated by image analysis and laser diffraction. Values for particle size distribution obtained by the two methods were different which is anticipated since the two methods measure different estimates of particle size. Equivalent circular diameters were measured by microscopy and volume diameters by laser diffraction. Consequently, these data should not be exactly equivalent. Their similarity confirms that the median size and distribution is within the designated size ranges.

The static angle of repose, moisture content, density and surface area were evaluated and data for the various powders are listed in Table II. Free flowing powders yield low static angles of repose, whereas high values are characteristic of powders exhibiting poor flow. Based on static angle of repose values obtained for sieved excipient particles (45–75 and 75–125 μm), the order of flow was sodium chloride > lactose > maltodextrin. The moisture content of the various powders ranged from 4.9 to 6.7%. Micronized albuterol sulfate particles consisted of loose aggregates and exhibited the lowest bulk and tapped densities (0.14 and 0.24 g/cm^3, respectively), whereas sodium chloride with rigid cubic crystals possessed the highest bulk and tapped density (1.39 and 1.52 g/cm^3, respectively, for 45–75 μm particles). Micronized albuterol sulfate exhibited

Table I. Particle Size and Distribution of the Various Powders as Determined by Scanning Electron Microscopy/Image Analysis and Laser Diffraction

Powder	Size range (μm)	Particle size and distribution			
		Image analysis[a]		Laser diffraction[b]	
		CMD (μm)	GSD	MD (μm)	GSD
Lactose	45–75	52.45	1.54	50.38 (0.57)	1.47 (0.05)
	75–125	98.47	1.59	78.38 (0.48)	1.67 (0.02)
Maltodextrin	45–75	58.56	1.58	38.26 (0.49)	1.69 (0.03)
	75–125	95.2	1.52	81.62 (0.34)	1.68 (0.02)
Sodium chloride	45–75	53.78	1.58	43.22 (0.47)	1.65 (0.04)
	75–125	115.42	1.46	110.32 (0.52)	1.59 (0.02)
Albuterol sulfate	<5	2.47	1.73	2.14 (0.32)	1.84 (0.03)

[a] The diameters of a minimum of 500 particles were measured.
[b] n = 5, values in parenthesis represent SDs.

the highest surface area per unit volume (11.735 m^2/g), and sodium chloride the lowest (0.072 m^2/g for 45–75 μm particles). Maltodextrin and lactose powders possessed intermediate density and surface area values.

The powders selected exhibited varying physico-chemical properties and studies were performed to evaluate their combined effects on bulk powder flow, particle detachment and aerosol dispersion.

Powder Flow

Beds of lactose and maltodextrin powder exhibited irregular or aperiodic oscillations of $d\theta$ versus time, whereas sodium chloride powder beds exhibited near periodic behavior. Phase-space plots of lactose and maltodextrin powders were characterized by repetitive, non-overlapping trajectories or attractors which is evidence of chaotic behavior. An attractor is defined as a series of trajectories in phase-space that never exactly repeat themselves and are attracted to each other around the origin. The diameter of the attractor or its distance from the origin reflects the deviation of θ from $\bar{\theta}$, whereas the relative proximity between adjacent trajectories of an attractor reflects the irregularity or non-repetitive nature of these deviations. Phase-space plots, characterized by repetitive patterns orbiting the origin, for 45–75 μm sodium chloride and lactose particles are shown in Fig. 1. The attractor for 45–75 μm lactose (poor flow) exhibited a larger diameter and divergence between adjacent trajectories in comparison to the sieved sodium chloride samples (superior flow) which were characterized by overlapping trajectories resembling a single loop in phase-space. The capacity dimensions of the various powders, defining the geometric dimension of these attractors in phase-space, are listed in Table III. A low capacity dimension is indicative of superior flow. The capacity dimensions for the three excipients ranged from 1.24 ± 0.01 for 45–75 μm sodium chloride (superior flow) to 1.82 ± 0.02 for 75–125 μm maltodextrin (poor flow) [n = 3]. Based on capacity dimensions, the order of flow was sodium chloride > lactose > maltodextrin.

Particle Detachment from Solid Surfaces

Impact forces in the range of 0.2–50 Newton (N) were achieved by varying the hammer weight and angle of release of the pendulum. The size of particles remaining on the disc following impact decreased with increasing impact force. A direct linear correlation (R^2 = 0.9912) existed between the size of particles adhered and the capacity dimensions (flow) of the excipient powders. This correlation is shown in Fig. 2, for an impact force of 1.21 N, and values of the particle size and distribution are listed in Table III. The size of adhered particles

Table II. Static Angle of Repose, Moisture Content, Density (Bulk and Tapped), and Surface Area of the Various Powders Evaluated

Powder	Size range (μm)	Static angle of repose[a] (degrees)	Moisture content[a] (%)	Density[a] (g/cm^3)		Surface area[b] (m^2/g)
				Bulk	Tapped	
Lactose	45–75	33.6 (0.5)	5.2 (0.1)	0.72 (0.02)	0.86 (0.03)	0.203 (0.009)
	75–125	30.5 (0.2)	5.3 (0.1)	0.73 (0.02)	0.88 (0.01)	0.184 (0.008)
Maltodextrin	45–75	34.6 (0.6)	6.4 (0.2)	0.57 (0.01)	0.69 (0.02)	0.152 (0.002)
	75–125	35.5 (0.3)	6.5 (0.1)	0.54 (0.01)	0.65 (0.01)	0.173 (0.008)
Sodium chloride	45–75	24.8 (0.3)	6.7 (0.1)	1.39 (0.03)	1.52 (0.03)	0.072 (0.006)
	75–125	24.6 (0.2)	6.4 (0.2)	1.34 (0.02)	1.48 (0.01)	0.068 (0.004)
Albuterol sulfate	<5	46.2 (0.3)	4.9 (0.1)	0.14 (0.01)	0.24 (0.02)	11.735 (0.750)

[a] n = 5, values in parenthesis represent SDs.
[b] n = 2, values in parenthesis represent the statistical range.

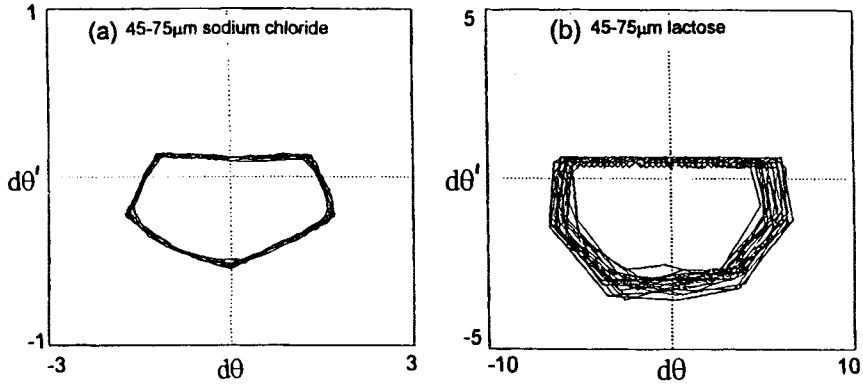

Fig. 1. Phase-space plots for (a) 45–75 μm sodium chloride, and (b) 45–75 μm lactose powders.

Table III. Data Indicating a Correlation Between Powder Flow, Particle Detachment, and *In Vitro* Aerosol Dispersion

Excipient	Size range (μm)	Capacity dimension[a]	Impact force (1.21N)[a] CMD(μm)	Impact force (1.21N)[a] GSD	Fine particle mass, FPM (μg) of albuterol sulfate blends[b] Rotahaler®	Fine particle mass, FPM (μg) of albuterol sulfate blends[b] Dry powder insufflator	Reduction in PIP[c] (%)
Lactose	45–75	1.52 (0.01)	21.04 (0.12)	1.67 (0.01)	102.9 (3.2)	123.4 (4.6) [HDE]	19.44 (4.46)
	75–125	1.59 (0.02)	25.14 (0.25)	1.71 (0.02)	94.2 (2.7)	—	—
Maltodextrin	45–75	1.74 (0.02)	29.73 (0.16)	1.71 (0.02)	24.7 (2.1)	—	—
	75–125	1.82 (0.01)	33.46 (0.38)	1.69 (0.02)	20.5 (2.0)	32.5 (3.1) [LDE]	5.82 (1.43)
Sodium chloride	45–75	1.24 (0.01)	13.14 (0.11)	1.69 (0.01)	135.9 (5.2)	—	—
	75–125	1.27 (0.02)	14.34 (0.24)	1.65 (0.02)	128.7 (3.5)	—	—

Note: Reduction in pulmonary inflation pressure (PIP) for selected formulations are also listed.
[a] n = 3.
[b] n = 5.
[c] n = 16, values in parenthesis represent SDs.

decreased with decreasing capacity dimensions (smaller irregularities in dynamic flow) of the powders, indicating enhanced detachment properties (small particle size cut-off for detachment) of particles exhibiting superior dynamic flow properties. The ease of particle detachment based on impact force separation measurements was sodium chloride > lactose > maltodextrin, which correlated with powder flow behavior.

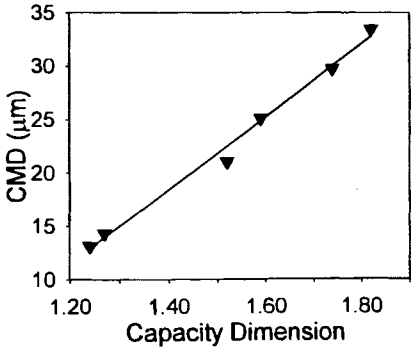

Fig. 2. Plots of the size of excipient particles (CMD, μm) adhered to the sapphire disc following impact (1.21 N) versus the capacity dimension, indicating a direct linear correlation (r^2 = 0.9912) between particle detachment and powder flow.

Aerosol Dispersion and *In Vitro* Aerodynamic Characterization

Based on *in vitro* aerosol delivery, the ease of dose delivery and FPM was as follows: sodium chloride > lactose > maltodextrin (Table III). This trend correlates with powder flow and particle detachment data.

Figure 3 shows a direct correlation (R^2 = 0.9741) between flow (capacity dimension) and dose delivery (FPM) for blends

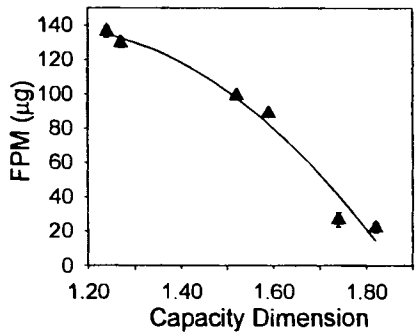

Fig. 3. Plots of capacity dimensions versus fine particle mass (FPM, μg) indicating a correlation (r^2 = 0.9741) between powder flow and aerosol dispersion.

delivered from the Rotahaler® at 60 L/min. Powders that exhibited poor flow (large capacity dimensions) experienced greater inter-particulate and particle-surface interactions, and hence, dispersed less readily as aerosols (lower FPM). A linear plot of the relationship between capacity dimensions and dispersion, with a maximum FPM of 1000 μg for an ideal free flowing powder, might be anticipated if flow was the only factor affecting FPM. However, the non-linearity in the data may be due to additional limitations in the delivery efficiency of the device resulting in much lower FPM values (~140 μg) for free flowing powders.

Statistical Experimental Design

The excipient, size range, and blend concentration had a statistically significant effect ($p < 0.05$) on FPM. The 2% albuterol sulfate blend in 45–75 μm lactose was identified as the highest dosing efficiency (HDE) formulation and the 1% blend in 75–125 μm maltodextrin as the lowest dosing efficiency (LDE) formulation. These two blends, at equivalent doses, were employed for pharmacodynamic evaluations.

Pharmacodynamic Evaluation

The dose recoveries and reproducibility as evaluated by the MDI unit dosage sampling device were acceptable as indicated by the high recoveries and low standard deviations for the two formulations: 98.94 ± 1.26% for the HDE and 97.76 ± 2.08% for the LDE formulation. Inertial impaction studies were performed on aerosols of the HDE and LDE formulations generated from a dry powder insufflator (used to administer aerosols to the guinea pig). Values of FPM are listed in Table III, and confirm a similar trend in dispersion properties as observed with the Rotahaler®.

Formulations, at equivalent doses and relative amounts, delivered to the guinea pig were as follows: A: 2% albuterol sulfate in 45–75 μm lactose (HDE, 5.0 mg = 100 μg of drug); B: 1% albuterol sulfate in 75–125 μm maltodextrin (LDE, 10 mg = 100 μg of drug); C: 45–75 μm lactose control (5.0 mg) and D: 75–125 μm maltodextrin control (10.0 mg). Sixteen guinea pigs were utilized in the study, each receiving all the above four treatments (A–D) in random order as defined by a 4 × 4 Latin square design. The time between successive treatments (approximately 45 min) was sufficient to allow for measurement of changes in PIP, and return of the PIP to normal baseline values. Studies were also performed in guinea pigs (n = 3) to evaluate the effect of anesthesia and experimental conditions on PIP over the entire duration of the study (approximately 4 hours). PIP was fairly constant and did not exhibit wide variations in baseline values.

A reduction in pulmonary inflation pressure (PIP) from baseline values was observed following administration of equivalent doses of albuterol sulfate dry powder aerosols. The results for selected formulations can be seen in Fig. 4. The largest (19.44 ± 4.46%) and smallest (5.82 ± 1.43%) reduction in PIP were obtained by the HDE (45–75 μm lactose, FPM = 123.4 ± 4.6 μg) and LDE (75–125 μm maltodextrin, FPM = 32.5 ± 3.1 μg) formulations, respectively. These differences could be attributed to greater peripheral rather than central airway deposition resulting from the ease of dispersion of lactose versus maltodextrin blends. Excipient controls resulted in small but insignificant effects on PIP (45–75 μm lactose = 0.44 ± 0.76%; 75–125 μm maltodextrin = 0.25 ± 0.48%). The differences between the two treatment groups and between each treatment and their respective controls were statistically significant ($p < 0.05$). Pharmacodynamic effect (PIP) plotted versus FPM can be seen in Fig. 5. Formulations that exhibited a higher *in vitro* dose delivery (higher FPM) resulted in a greater reduction in PIP. Excipient controls exhibited insignificant effects. These studies demonstrated a proportionality between % reduction in PIP and FPM, but additional formulations need to be evaluated before a correlation can be drawn.

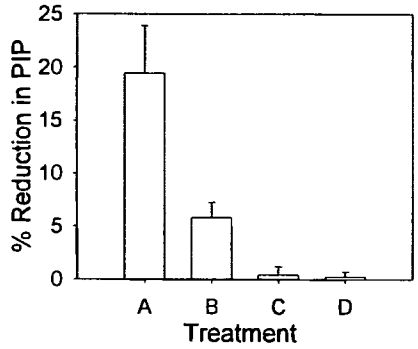

Fig. 4. Plots of percent reduction in pulmonary inflation pressure (PIP) from baseline values for the treatments and excipient controls evaluated. A: highest dosing efficiency (HDE) formulation, FPM = 123.4 ± 4.6 μg; B: lowest dosing efficiency (LDE) formulation, FPM = 32.5 ± 3.1 μg; C: 45–75 μm lactose; D: 75–125 μm maltodextrin.

CONCLUSIONS

Novel techniques for analyzing dynamic powder flow properties have been developed. Drug and excipient particles in size ranges suitable for dry powder aerosol delivery to the lungs were evaluated using these techniques. Striking direct relationships between powder flow properties, particle detachment, and aerosol dispersion were observed with implications for pharmacodynamic effect (Table III).

The key numerical descriptor of powder flow, the capacity dimension, was generated from novel chaos analysis of dynamic

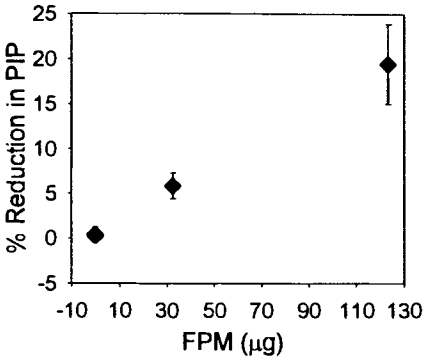

Fig. 5. Percent reduction in pulmonary inflation pressure plotted versus fine particle mass indicating a proportionality between *in vitro* aerosol dispersion and *in vivo* pharmacodynamic effect. Formulations that exhibited a higher *in vitro* dose delivery resulted in a greater reduction in pulmonary inflation pressure. Excipient controls resulted in small but insignificant effects on PIP.

angle of repose data. A low capacity dimension was indicative of superior flow. A pendulum impact force separation device was designed to evaluate particle detachment from solid surfaces. Ease of particle separation (small particle size cut-off for detachment) correlated directly ($r^2 = 0.9912$) with flow. Dry powder aerosol delivery from the Rotahaler® indicated a direct proportionality ($r^2 = 0.9741$) between flow and dispersion (FPM). Powders exhibiting poor flow (large capacity dimensions) dispersed less readily (low FPM). For the three excipients evaluated, the order of powder flow, particle detachment and *in vitro* dose delivery was sodium chloride > lactose > maltodextrin. An experimental design identified the highest and lowest *in vitro* dosing efficiency formulations for pharmacodynamic evaluation of bronchodilation in guinea pigs. *In vivo* studies demonstrated a proportionality between PIP and FPM.

These methodologies integrated various levels of *in vitro* powder behavior, and addressed the hypothesis that numerical descriptors of powder flow predict dry powder aerosol dispersion. Preliminary pharmacodynamic evaluations demonstrated the potential of these techniques to evaluate a correlation between *in vitro* powder properties and *in vivo* effect.

Understanding the key features and the relationships among physico-chemical particle attributes, flow behavior, aerosol dispersion and ultimately pharmacodynamic effect, may allow preferential selection of a specific powder from several available powders, in preformulation design, and holds promise for broad-based use in the development of pharmaceutical formulations.

ACKNOWLEDGMENTS

The authors would like to thank GlaxoWellcome Inc., RTP, NC, for funding this project, and the Physics Instrument Shop, UNC-CH, for constructing the dynamic angle of repose and impact force separation devices to their design specifications.

REFERENCES

1. A. R. Clark. Medical aerosol inhalers: past, present and future. *Aerosol Sci. and Tech.* **22**:374–391 (1995).
2. S. P. Newman and S. W. Clarke. Therapeutic aerosols, I, physical and practical considerations. *Thorax.* **38**:881–886 (1983).
3. G. Scheuch and W. Stahlhofen. Deposition and dispersion of aerosols in the airways of the human respiratory tract: the effects of particle size. *Exp. Lung Res.* **18**:343–358 (1992).
4. S. P. Newman. In S. W. Clark and D. Pavia (eds), *Aerosols and the Lung: Clinical and Experimental Aspects*, Butterworths, London, 1984, pp. 197–224.
5. P. J. Davies, G. W. Hanlon, and A. J. Molyneux. An investigation into the deposition of inhalation aerosol particles as a function of air flow rate in a modified Kirk lung. *J. Pharm. Pharmacol.* **28**:908–911 (1976).
6. J. Visser. An invited review: Van der Waals and other cohesive forces affecting powder fluidization. *Powder Tech.* **58**:1–10 (1989).
7. A. J. Hickey, N. M. Concessio, M. M. VanOort, and R. M. Platz. Factors influencing the dispersion of dry powders as aerosols. *Pharm. Tech.* **18**:58–64 (1994).
8. N. M. Concessio. Dynamic properties of pharmaceutical powders and their impact on aerosol dispersion, thesis, University of North Carolina at Chapel Hill (1997).
9. A. J. Hickey and N. M. Concessio. Flow properties of selected pharmaceutical powders from a vibrating spatula. *Part. Part. Syst. Charac.* **11**:457–462 (1994).
10. P. Speiser and R. Tawashi. Misch wirkung Pharmazeutisch ver wendeter Pulvermischer. *Pharm. Acta. Helv.* **37**:529–543 (1962).
11. J. T. Carstensen. *Pharmaceutical Principles of Solid Dosage Forms*, Technomic Publishing Company, Lancaster, 1993.
12. A. J. Hickey and N. M. Concessio. Chaos in rotating lactose powder beds. *Particulate Sci. and Tech.* **14**:15–25 (1996).
13. N. M. Concessio and A. J. Hickey. Analysis of the patterns of particle dispersion from a dry powder inhaler. *Pharm. Tech.* **20**:50–62 (1996).
14. A. J. Hickey and N. M. Concessio. Descriptors of irregular particle morphology and powder properties. *Adv. Drug Del. Rev.* **26**:29–40 (1997).
15. F. C. Moon. *Chaotic and Fractal Dynamics*, John Wiley and Sons, New York, 1992.
16. D. Ruelle. Strange attractors. *Math Intelligencer* **2**:126–137 (1980).
17. B. Kaye. *Chaos and Complexity: Discovering the Surprising Patterns of Science and Technology*, VCH Publishers, New York, 1993, pp. 64–70.
18. H. Froehling, J. P. Crutchfield, D. Farmer, N. H. Packard, and R. Shaw. On determining the dimension of chaotic flows. *Physica.* **3D**:605–617 (1981).
19. J. D. Farmer, E. Ott, and J. A. Yorke. The dimension of chaotic attractors. *Physica.* **7D**:153–180 (1983).
20. A. Otsuka, K. Kida, K. Danjo, and H. Sunada. Measurement of the adhesive force between particles of powdered organic materials and a glass substrate by means of the impact separation method, I, effect of temperature. *Chem. Pharm. Bull.* **31**:4483–4488 (1983).
21. B. A. Webber, J. V. Collins, and M. A. Braithewaite. Sever acute asthma: a comparison of three methods of inhaling Salbutamol. *Br. J. Dis. Chest.* **76**:69–74 (1982).
22. B. S. Cohen. The first 40 years. In J. P. Lodge and T. L. Chan (eds), *Cascade Impactor, Sampling and Data Analysis*, American Industrial Hygiene Assoc., Ohio, 1986.
23. J. P. Mitchell, P. A. Costa, and S. Waters. An assessment of an Andersen Mark-II cascade impactor. *J. Aerosol Sci.* **19**:231–221 (1988).
24. R. M. Auty, K. Brown, M. Neale, and P. D. Snashall. Respiratory tract deposition of sodium cromoglycate is highly dependent upon technique of inhalation using the Spinhaler. *Br. J. Dis. Chest.* **81**:371–380 (1987).
25. M. VanOort, B. Downey, and W. Roberts. Verification of operating the Andersen cascade impactor at different flow rates. *Pharm. Forum.* **22**:2211–2215 (1996).
26. N. M. Concessio, R. Jager-Waldau, and A. J. Hickey. Aerosol delivery from an active emission multi-single dose dry powder inhaler. *Particulate Sci. Tech.* **15**:51–63 (1997).
27. S. Desquand, J. Lefort, C. Dumarey, and B. B. Vargaftig. The booster injection of antigen during active sensitization of guinea pig modifies the anti-anaphylactic activity of the PAF antagonist WEB 2086. *Br. J. Pharmacol.* **100**:217–222 (1990).
28. D. A. Handley, J. J. DeLeo, and A. M. Havill. Induction of aerosol allergen of sustained and nonspecific IgE-mediated airway hyperactivity in the guinea pig. *Agents Actions.* **37**:201–203 (1992).
29. H. Konzett and R. Roessler. Versuchsanordnung zu untersuchungen an der Bornchialmuskulatur. Naunyn Schmiedeberg. *Arch. Exp. Path. Pharmakol.* **195**:71–74 (1940).
30. J. S. Franzone, R. Cirillo, and P. Biffignandi. Doxofylline exerts a prophylactic effect against bronchoconstriction and pleurisy induced by PAF. *Eur. J. Pharmacol.* **165**:269–277 (1989).